INTERNATIONAL JOURNAL OF APPLIED BIOLOGY AND PHARMACEUTICAL TECHNOLOGY

www.ijabpt.com Volume-5, Issue-4, Oct-Dec-2014 Coden : IJABPT Copyrights@2014

ISSN : 0976-4550

Received: 10th July-2014 *Revised: 3rd Aug-2014* *Accepted: 16th Aug-2014*

Research article

HOMOLOGY MODELLING AND DOCKING STUDIES OF PLANT DERIVED NATURAL COMPOUNDS ON STAPHYLOCOCCUS AUREUS

S.Anitha

Department of Biotechnology, Sri Krishnadevaraya University, Anantapur, A.P.India

ABSTRACT: Staphylococcus aureus avoid innate immune responses including phagocytosis is crucial for the organism to cause infection. This process involves several secreted and cell-surface-associated proteins. In this study I identified the action of plant compounds on Iron regulated surface protein using docking studies with homology modeled Surface protein. Through the modeled protein, the flexible Docking study was performed with plant derived compounds with theoretically predicted active sites. The results indicated that amino acid CYS-88, TYR-112 and LEU-113 present in Iron regulated surface protein are core important for binding activities and these residues are having strong hydrogen bond interactions with compounds. I have investigated the plant derived compounds like vannillic interactions and scoring parameters in GOLD, and the GOLD score results are interesting. Our results may be helpful for further investigations in both in vivo and in vitro conditions.

Key words: Iron regulated surface protein, Modeller7v7; Molecular docking; Staphylococcus aureus.

INTRODUCTION

Methicillin resistant Staphylococcus aureus (MRSA) is the term used for bacteria of the *Staphylococcus aureus* group (*S. aureus*) that are resistant to the usual antibiotics used in the treatment of infections with such organisms [1, 2]. Traditionally MRSA stood for methicillin (meticillin) resistance but the term increasingly refers to a multi-drug resistant group [3, 4]. Such bacteria often have resistance to many antibiotics traditionally used against *S.aureus*. This resistance to methicillin is due to the presence of the *mec* gene in the bacteria [5]. This alters the site at which methicillin binds to kill the organism. Hence, methicillin is not able to effectively bind to the bacteria. Infections caused by MRSA are the same as other staphylococcal infections because the organism itself is not any more virulent (or infectious) than usual type *S.aureus [6]*. Like other *S.aureus*, MRSA can colonise the skin and body of an individual without causing sickness, and in this way it can be passed on to other individuals unknowingly. Problems arise in the treatment of overt infections with MRSA because antibiotic choice is very limited [7,8]. MRSA is found worldwide, predominantly in hospitals and institutions such as nursing homes. Much less commonly, MRSA is found in the general community. There are three main reservoirs (and hence sources of spread and infection) for MRSA in hospital and institutions: staff, patients and inanimate objects such as beds, linen and utensils. By far the most important reservoir is patients who may be colonised with MRSA without evidence of infection [9]. The usual sites of colonisation with MRSA are the nostrils, skin, groin, axilla, and wounds. Most health professionals who are colonised with MRSA do not develop infection and many spontaneously clear the organism without treatment [10]. Once colonisation has been present for more than three months, it becomes much more difficult to clear [11]. Patients, however, have a 30-60% risk of infection following colonisation [12]. This is probably due to factors related to the illness for which they are hospitalised, which impair their ability to clear or control colonisation with the organism [13]. Most MRSA infections occur in wounds (e.g. surgical wounds), skin (e.g. intravenous access sites), or in the bloodstream. Mortality from these infections is not significantly different from those seen with usual type *S.aureus* infections.

METHODOLOGY

The initial model of Iron-regulated surface determinant protein was built by using homology-modeling methods and the MODELLER software. The sequence of Iron-regulated surface determinant protein was obtained from Uniprot. The query sequence from *Staphylococcus* was submitted to domain fishing server for Iron-regulated surface determinant protein domain prediction. The predicted domain *was* searched to find out the related protein structure to be used as a template by the BLAST (Basic Local Alignment Search Tool) program against PDB (Protein Data bank).

Sequence that showed maximum identity with high score and less e-value was aligned and was used as a reference structure to build a 3D model for Iron-regulated surface determinant protein. The co-ordinates for the structurally conserved regions (SCRs) for Iron-regulated surface determinant protein were assigned from the template using multiple sequence alignment, based on the Needleman-Wunsch algorithm. Finally, the structure having the least energy with low RMSD (Root Mean Square Deviation) was used for further studies. In this step, the quality of the initial model was improved.The final structure obtained was analyzed by Ramachandran's map using PROCHECK (Programs to check the Stereo chemical Quality of Protein Structures) and environment profile using ERRAT graph (Structure Evaluation server). This model was used for the identification of active site and for docking of the substrate with the enzyme.

Active site Identification

Active site of Iron-regulated surface determinant protein was identified using CASTp server. A new program, CASTp, for automatically locating and measuring protein pockets and cavities, is based on precise computational geometry methods, including alpha shape and discrete flow theory. CASTp identifies and measures pockets and pocket mouth openings, as well as cavities. The program specifies the atoms lining pockets, pocket openings, and buried cavities; the volume and area of pockets and cavities; and the area and circumference of mouth openings.

Docking method

Docking with GOLD 3.0.1

GOLD (Genetic Optimization of Ligand Docking) a genetic algorithm (GA) based software, mainly utilizes an evolutionary strategy involving 3 genetic operators; cross overs, mutations and migrations. GOLD imports the partial flexibility to proteins and full flexibility to inhibitors. The compounds are docked into the active site of Iron-regulated surface determinant protein and the interaction of these ligands with the active site residues are thoroughly studied using calculations of molecular mechanics. The parameters used for GA were population size (100), selection pressure (1.1), number of operations (10,000), number of island (1) and niche size. Operator parameters for crossover, mutation and migration were set to 100, 100 and 10 respectively. Default cutoff values of 3.0A° (dH-X) for hydrogen bonds and 6.0A° for vanderwaals were employed. The default algorithm speed was selected and the inhibitor binding site in Iron-regulated surface determinant protein were defined within a 10A° radius with the centroid as HH atom of TYR51, HIS13, GLN8 respectively. The number of poses for each inhibitor was set 100, and early termination was allowed if the top three bound conformations of inhibitors were within 1.5A° RMSD. After docking, the individual binding poses of each inhibitor were observed and their interactions with the protein were studied. The best and most energetically favorable conformation of each inhibitor was selected.

GOLD Score fitness function

The four components vig, Protein-ligand hydrogen bond energy (external H-bond); Protein-ligand vanderwaals energy (external vdw); Ligand internal vanderwaals energy (internal vdw); and Ligand intramolecular hydrogen bond energy (internal- H- bond) were considered for calculating the fitness function of GOLD score. The protein-ligand hydrophobic contact was encouraged by making an empirical correction by multiplying external vdw score with 1.375. The fitness function has been optimized for the prediction of ligand binding positions.

Gold Score = S (hb_ext) + S (vdw_ext) + S (hb_int) + S (vdw_int)

Where S (hb_ext) is the protein-ligand hydrogen bond score, S (vdw_ext) is the protein-ligand vanderwaals score, S (hb_int) is the score from intramolecular hydrogen bond in the ligand and S (vdw_int) is the score from intramolecular strain in the ligand.

RESULTS AND DISCUSSION

Homology Modelling of Iron-regulated surface determinant protein

A high level of sequence identity should guarantee more accurate alignment between the target sequence and template structure. In the results of BLAST search against PDB, only the 4FC3 which has a high level of sequence identity with the Iron-regulated surface determinant protein. Structurally conserved regions (SCRs) for the model and the template were determined by superimposition of the two structures and multiple sequence alignment.

```
domain          ----------------------DKDHSAPNSRPIDFEMKKKDGTQQFYHYASSVKPARVIFT 40
temp            QQYPPADESLQDAIKNPAIIDKEHTADNWRPIDFQMKNDKGERQFYHYASTVEPATVIFT 60
                                     **:*:* * *****:**:..* :*******:*:** ****

domain          DSKPEIELGLQSGQFWRKFEVYEGDKKLPIKLVSYDTVKDYAYIRFSVSNGTKAVKIVSS 100
temp            KTGPIIELGLKTASTWKKFEVYEGDKKLPVELVSYDSDKDYAYIRFPVSNGTREVKIVSS 120
                .:  * *****::.. *:************::*****: ********.*****: ******

domain          THF-NNKEEKYDYTLMEFAQPIYNSADKFKT 130
temp            IEYGENIHEDYDYTLMVFAQPITN------- 144
                 .: :* .*.****** ***** *
```

Fig 1: CLUSTAL 2.0.3 multiple sequence alignment

In the following study, we have chosen 4FC3 as a reference structure for modeling Iron-regulated surface determinant protein domain. Coordinates from the reference protein (4FC3) to the SCRs, structurally variable regions (SVRs), N-termini and C-termini were assigned to the target sequence based on the satisfaction of spatial restraints. In the modeller we will get a 20 PDB out of which we select a least energy. The energy unit will be in kilo joule. All side chains of the model protein were set by rotamers. The final stable structure of the Iron-regulated surface determinant protein obtained.

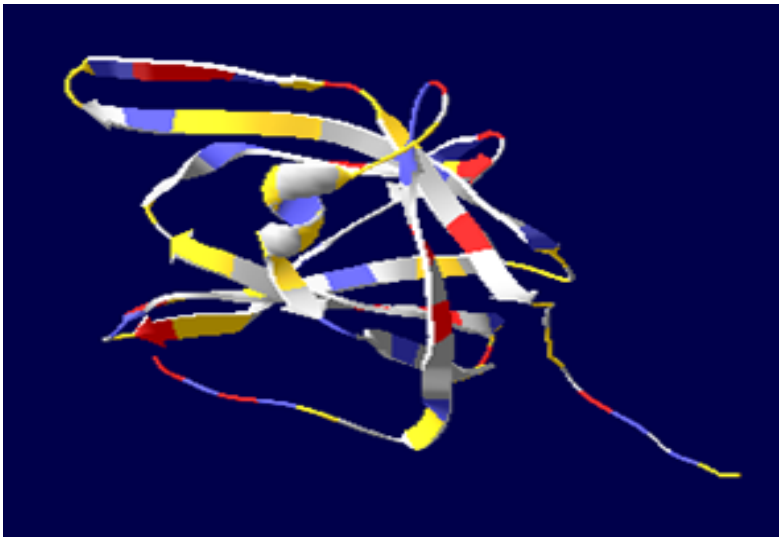

Figure 2. Modeller result

By the help of SPDBV it is evident that Iron-regulated surface determinant protein has 6 helices and 12 sheets and it is shown in the Figure 2.

The final structure was further checked by verify3D graph and the results have been shown in Figure 3: The overall scores indicates acceptable protein environment.

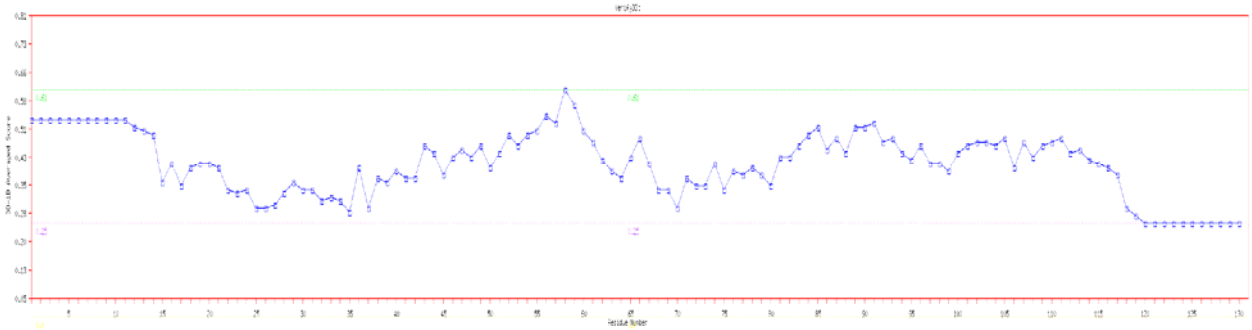

Figure 3: The 3D profiles verified results of Iron-regulated surface determinant protein model; overall quality score indicates residues are reasonably folded

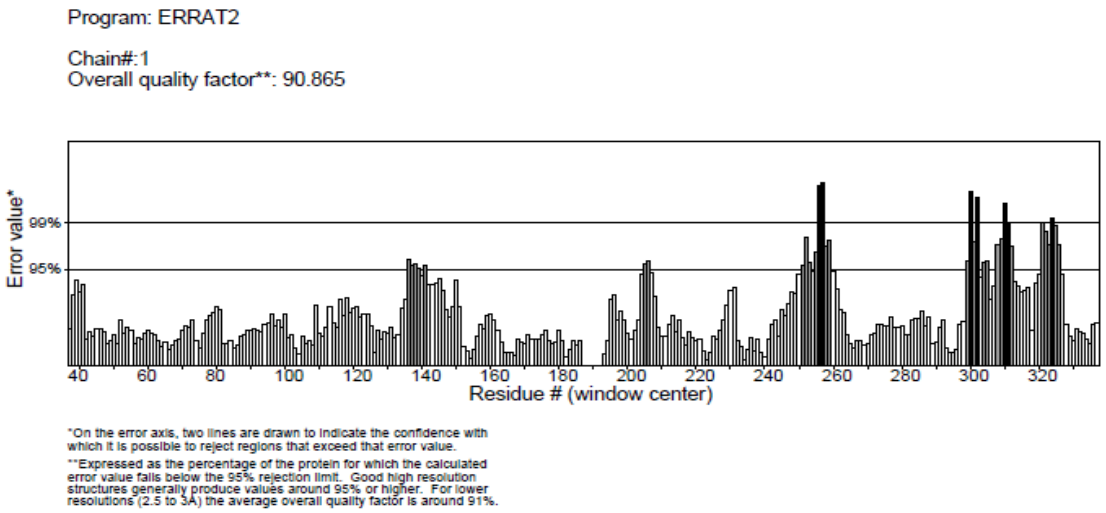

Figure 4: Errat result

Validation of Iron-regulated surface determinant protein Domain

After the refinement process, validation of the model was carried out using Ramachandran plot calculations computed with the PROCHECK program. The psi and pi distributions of the Ramachandran plots of non-glycine, non-proline residues are summarized. The RMSD (Root Mean Square deviation) deviation for covalent bonds and covalent angles relative to the standard dictionary of Iron-regulated surface determinant protein was -5.27 and -0.55 Å. Altogether 90.8 % of the residues of Iron-regulated surface determinant protein was in favored and allowed regions. The overall PROCHECK G-factor of Iron-regulated surface determinant protein was – 2.32 and verify3D environment profile was good.

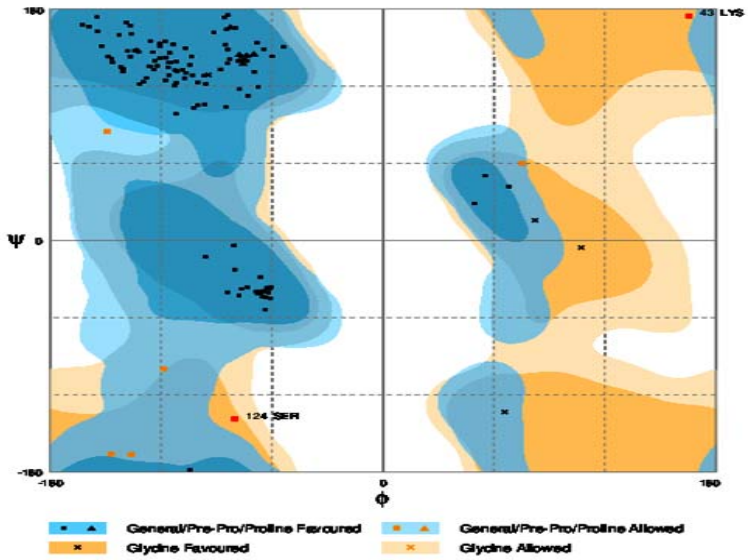

Figure 5: Ramachandran Plot

Number of residues in favoured region : 121 (94.5%)
Number of residues in allowed region : 5 (3.9%)
Number of residues in outlier region : 2 (1.6%)

Superimposition of 4FC3 with Iron-regulated surface determinant protein

The structural superimposition of 4FC3 template and Iron-regulated surface determinant protein is shown in Figure 6. The weighted root mean square deviation of trace between the template and final refined models 0.52A^{o}. This final refined model was used for the identification of active site and for docking of the substrate with the domain.

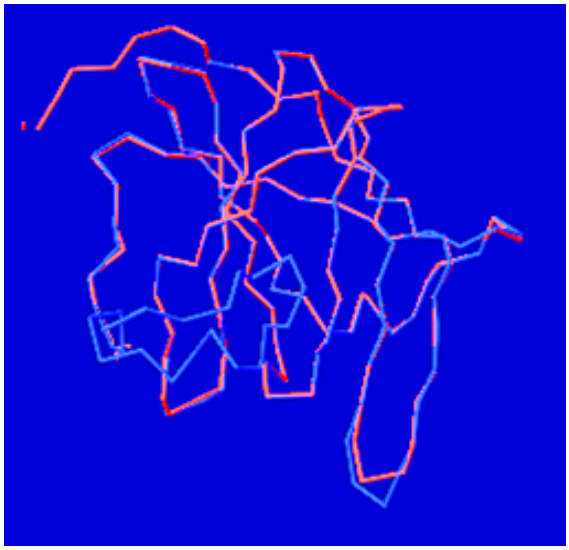

Figure 6: superimposition of C alpha trace of Iron-regulated surface determinant protein (represented in RED color) and 4FC3 (represented in BLUE color)

Active site Identification of Iron-regulated surface determinant protein

After the final model was built, the possible binding sites of Iron-regulated surface determinant protein was searched based on the structural comparison of template and the model build and also with CASTP server and was shown in Figure 7. It was found that secondary structures are highly conserved and the residues, ASP-65, CYS-66, CYS-88, TYR-112, LEU-113, LEU-115, ASP-117, ILE-118, GLN-136.

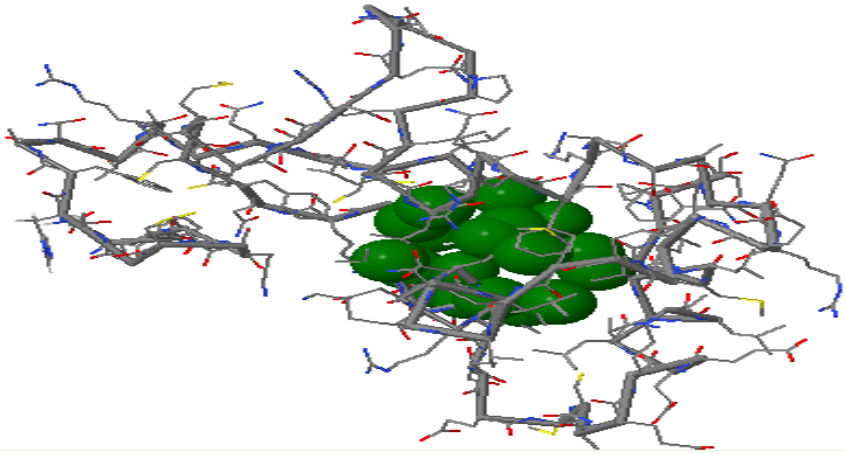

Figure 7: Active site of Iron-regulated surface determinant protein

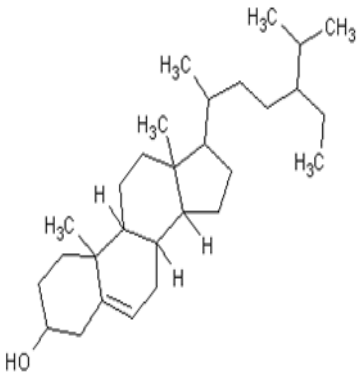

Molecular Formula = $C_{29}H_{50}O$

1. beta-sitosterol

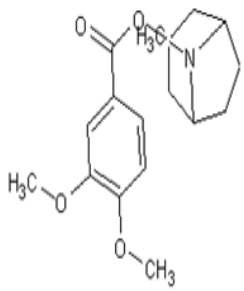

Molecular Formula = $C_{17}H_{23}NO_4$

2. Convolamine

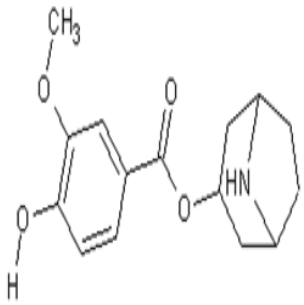

Molecular Formula = $C_{15}H_{19}NO_4$

3. Convolidine

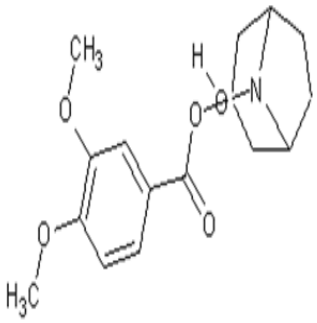

Molecular Formula = $C_{16}H_{21}NO_5$

4. Convoline

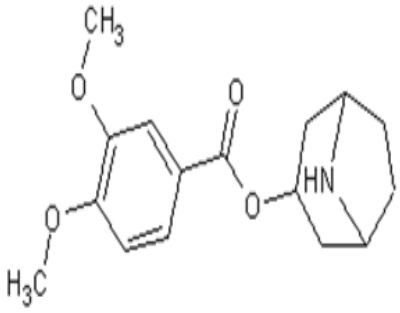

Molecular Formula = $C_{16}H_{21}NO_4$

5. Convolvine

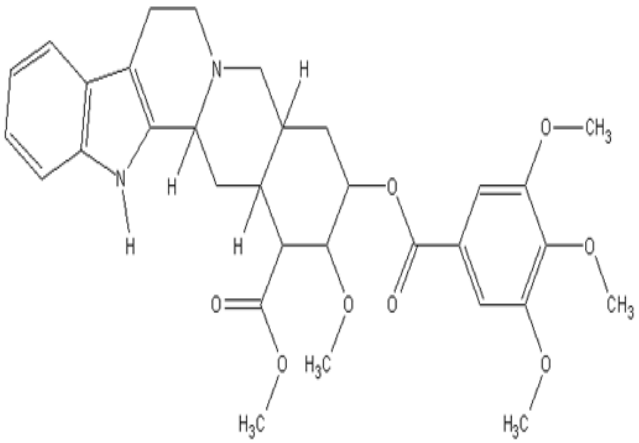

Molecular Formula = $C_{32}H_{38}N_2O_8$

6. Deserpidine

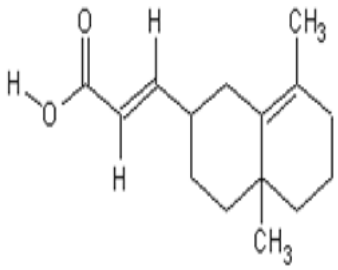

Molecular Formula = $C_{15}H_{22}O_2$

7. Macrophyllic acid

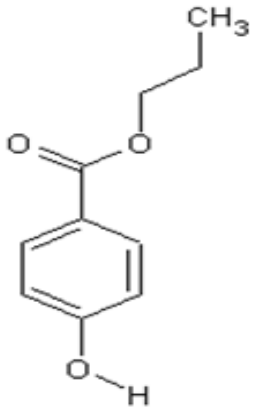

8. p-hydroxybenzoic

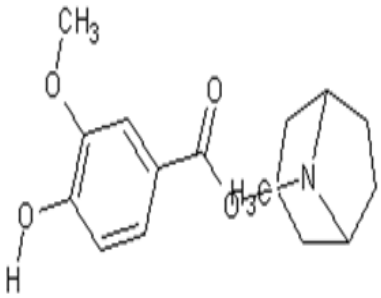

9. Phyllabine

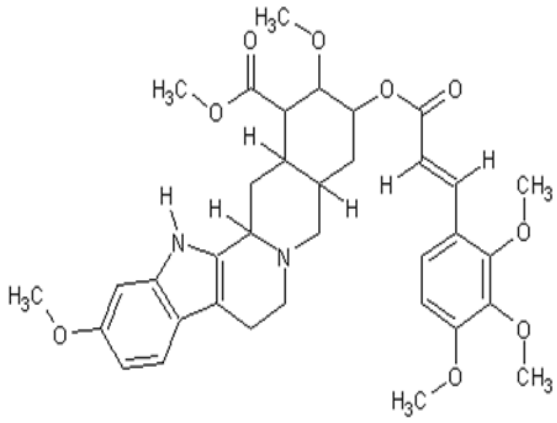

10. Rescinnamine

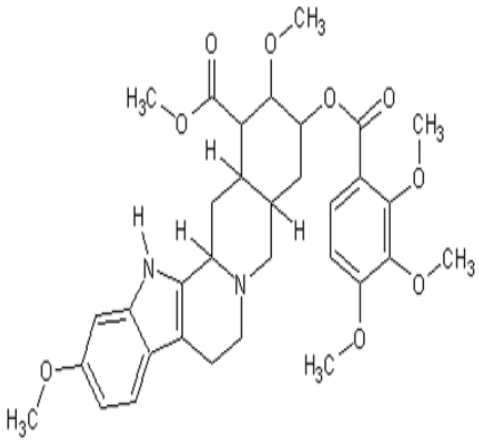

11. Reserpine

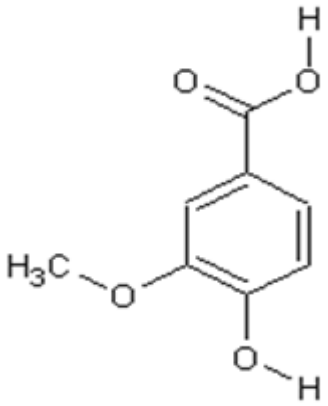

12. Vanillic

Fig 8: The inhibitors used for docking

The Chemical properties of these Structures are tabulated as Follows:

Table 1: Properties of Compounds

S.No	Molecular Formula	Formula Weight	Molar Refractivity(cm^3)	Index of refraction	Density(g/cm^3)
1	$C_{29}H_{50}O$	414.7067	129.21±0.4	1.521±0.03	0.97±0.1
2	$C_{17}H_{23}NO_4$	305.36882	82.74±0.4	1.560±0.03	1.19±0.1
3	$C_{15}H_{19}NO_4$	277.31566	73.04±0.4	1.592±0.03	1.28±0.1
4	$C_{16}H_{21}NO_5$	307.34164	79.64±0.4	1.587±0.03	1.29±0.1
5	$C_{16}H_{21}NO_4$	291.34224	77.88±0.4	1.560±0.03	1.21±0.1
6	$C_{32}H_{38}N_2O_8$	578.65272	154.57±0.4	1.625±0.03	1.32±0.1
7	$C_{15}H_{22}O_2$	234.33398	68.41±0.4	1.533±0.03	1.06±0.1
8	$C_{10}H_{12}O_3$	180.20048	49.17±0.3	1.531±0.02	1.134±0.06
9	$C_{16}H_{21}NO_4$	291.34224	77.90±0.4	1.590±0.03	1.26±0.1
10	$C_{35}H_{42}N_2O_9$	634.71598	170.10±0.4	1.621±0.03	1.31±0.1
11	$C_{33}H_{40}N_2O_9$	608.6787	160.93±0.4	1.619±0.03	1.32±0.1
12	$C_8H_8O_4$	168.14672	41.74±0.3	1.585±0.03	1.351±0.06

Docking of inhibitors with the active site of Iron-regulated surface determinant protein

Docking of the inhibitors given in Figure 6 with Iron-regulated surface determinant protein was performed using GOLD, which is based on Rigid Body Shape-Fitting. This program generates an ensemble of different rigid body orientations (poses) for each compound conformer within the binding pocket and then passes each molecule against a negative image of the binding site. Poses clashing with this 'bump map' are eliminated. Poses surviving the bump test are then scored and ranked with a Gaussian shape function. We defined the binding pocket using the ligand-free protein structure and a box enclosing the binding site. This box was defined by extending the size of a cocrystalized ligand by 4 Å. This dimension was considered here appropriate to allow, for instance, compounds larger than the cocrystallized ones to fit into the binding site. One unique pose for each of the best-scored compounds was saved for the subsequent steps. The compounds used for docking was converted in 3D with OMEGA. To this set, the substrate (generation of multiconformer with Omega) corresponding to the modeled protein were added.

Table 2: Docking Results

Fitness	S(hb_ext)	S(vdw_ext)	S(hb_int)	S(int)	File name
-21.25	0.00	30.03	0.00	-62.54	Betasitosterol
28.50	0.00	24.43	0.00	-5.10	Convolamine
32.25	1.89	26.31	0.00	-5.81	Convolidine
40.02	13.62	25.52	0.00	-8.68	Convoline
27.85	6.71	19.35	0.00	-5.46	Convolvine
38.01	5.50	36.74	0.00	-18.00	Deserpidine
20.37	0.00	26.48	0.00	-16.04	Macrophyllic acid
32.12	6.00	20.68	0.00	-2.32	p-hydroxybenzoic
28.89	0.00	24.66	0.00	-5.01	Phyllabine
28.60	0.18	40.22	0.00	-26.89	Rescinnamine
29.89	0.40	35.49	0.00	-19.31	Reserpine
27.24	6.00	17.64	0.00	-3.02	Vanillic

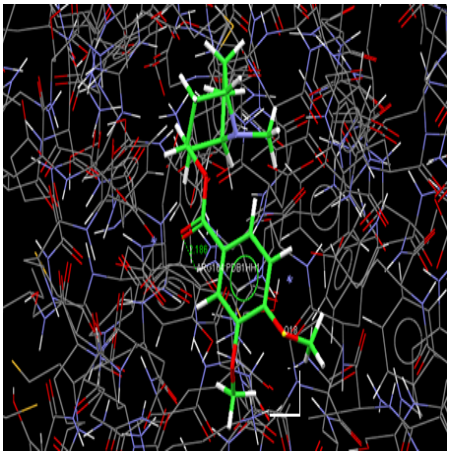

Betasitosterol

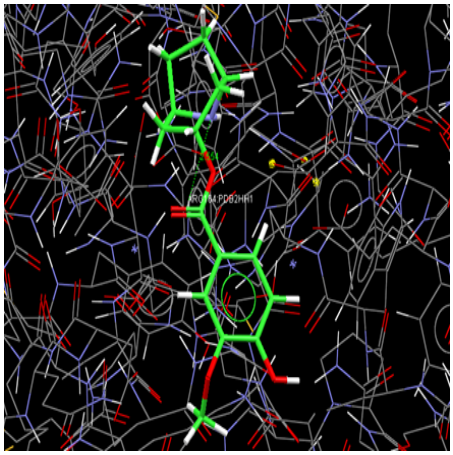

Convolamine

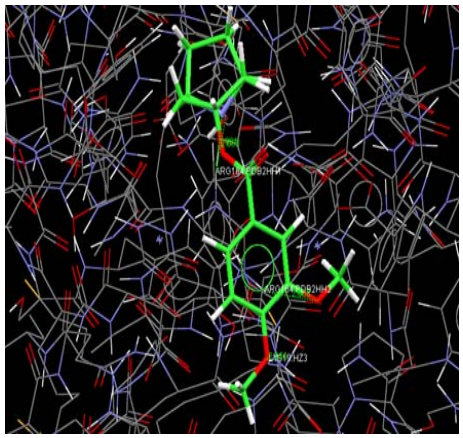

Convolidine

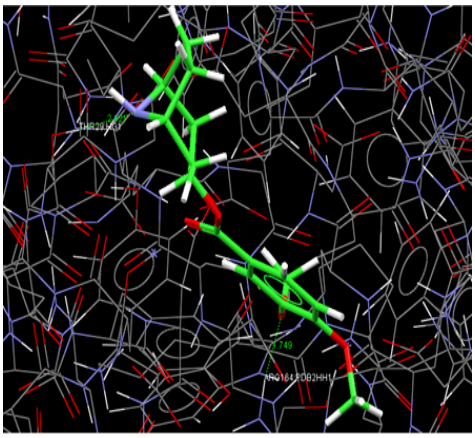

Convoline

Fig 9: Docking results

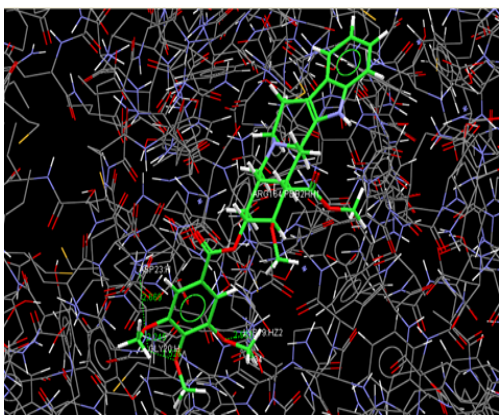

Convolvine

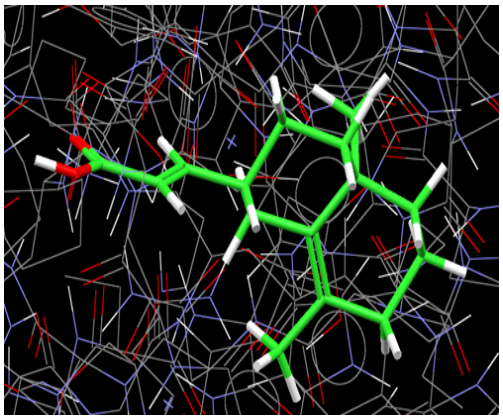

Deserpidine

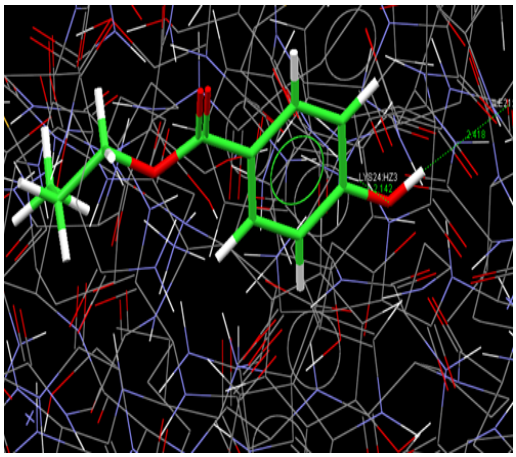

Macrophyllic acid

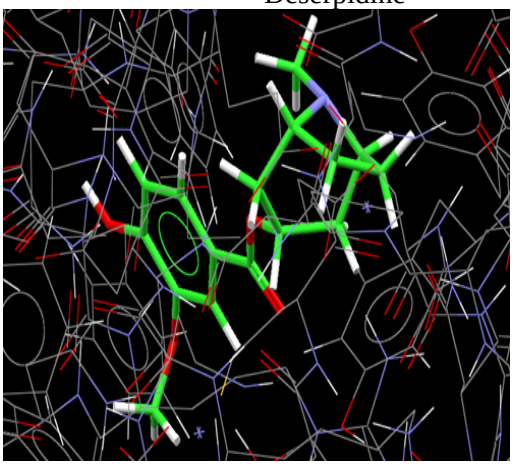

p-hydroxybenzoic

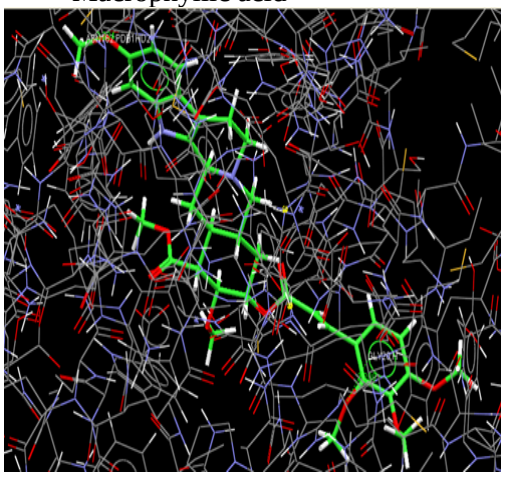

Phyllabine

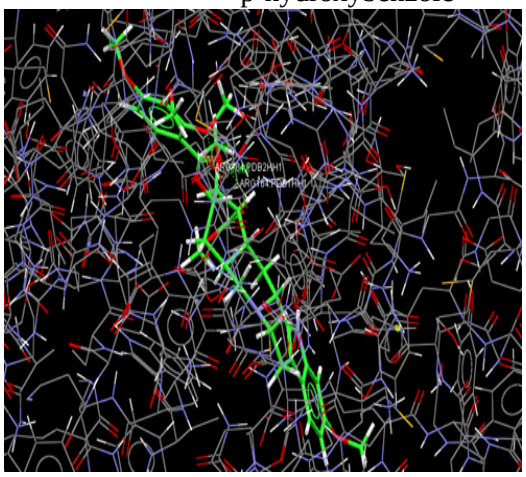

Rescinnamine

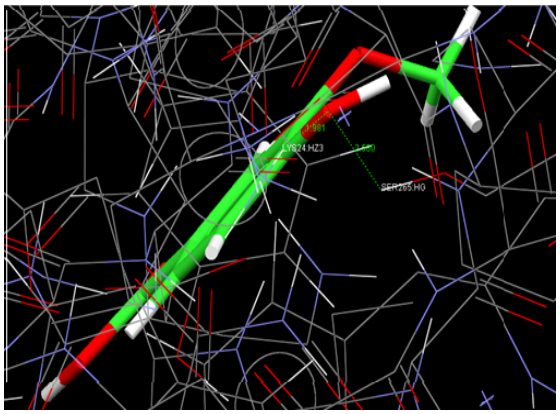

Vanillic

CONCLUSION

The compounds from medicinal plants were screened for the AntiMRSA activity. For this study the medicinal plants used are Celastrus paniculatus, Withania somnifera, Convolvulus pluricaulis, Rauvoifia Serpentina. Among many terpinoids, flavones and alkaloids we identified 12 compounds which have AntiMRSA property. These were screened and docked to the proteins like Iron-regulated surface determinant protein which is expressed cell membrane. Docking results shows that out of 12 Compunds, randomly 10 compunds were shown best docking energy to the Iron-regulated surface determinant protein, By this we can say that the above docked compunds may show the antistress activity.

REFFERENCES

Ahearn DJ, Jackson TB, McIlmoyle J, Weatherburn AJ. (2010). Improving end of life care for nursing home residents: an analysis of hospital mortality and readmission rates. Postgrad Med J. 86(1013):131-5

Baldwin NS, Gilpin DF, Hughes CM, Kearney MP, Gardiner DA, Cardwell C, (2009). Prevalence of methicillin-resistant Staphylococcus aureus colonization in residents and staff in nursing homes in Northern Ireland. J Am Geriatr Soc. 57(4):620-6.

Bocher S, Gervelmeyer A, Monnet DL, Molbak K, Skov RL, Danish (2008). CA-MRSA Study Group. Methicillin-resistant Staphylococcus aureus: risk factors associated with community-onset infections in Denmark. Clin Microbiol Infect. 14(10):942-8

Cox RA, Bowie PE. (1999). Methicillin-resistant Staphylococcus aureus colonization in nursing home residents: a prevalence study in Northamptonshire. J Hosp Infect. 43(2):115-22.

De Boer E, Zwartkruis-Nahuis JT, Wit B, Huijsdens; XW, de Neeling AJ, Bosch T, (2009). Prevalence of methicillin-resistant Staphylococcus aureus in meat. Int J Food Microbiol. 134(1-2):52-6.

Moore CL, Hingwe A, Donabedian SM, Perri MB, Davis SL, Haque NZ, (2009). Comparative evaluation of epidemiology and outcomes of methicillin-resistant Staphylococcus aureus (MRSA) USA300 infections causing community- and healthcare-associated infections. Int J Antimicrob Agents. 34(2):148-55.

Nemati M, Hermans K, Lipinska U, Denis O, Deplano A, Struelens M, (2008). Antimicrobial resistance of old and recent Staphylococcus aureus isolates from poultry: first detection of livestock-associated methicillin-resistant strain ST398. Antimicrob Agents Chemother. 52(10):3817-9.

Skov RL, Jensen KS. (2009). Community-associated meticillin-resistant Staphylococcus aureus as a cause of hospital-acquired infections. J Hosp Infect. 73(4):364-70.

Suetens C, Niclaes L, Jans B, Verhaegen J, Schuermans A, Van Eldere J, (2006). Methicillin-resistant Staphylococcus aureus colonization is associated with higher mortality in nursing home residents with impaired cognitive status. J Am Geriatr Soc. 54(12):1854-60.

Talon D, Woronoff-Lemsi MC, Limat S, Bertrand X, Chatillon M, Gil H, (2002). The impact of resistance to methicillin in Staphylococcus aureus bacteremia on mortality. Eur J Intern Med. 13(1):31-36.

Tenover FC, Goering RV. (2009). Methicillin-resistant Staphylococcus aureus strain USA300: origin and epidemiology. J Antimicrob Chemother. 64(3):441-6.

Van Rijen MM, Van Keulen PH, Kluytmans JA. (2008). Increase in a Dutch hospital of methicillin-resistant Staphylococcus aureus related to animal farming. Clin Infect Dis. 46(2):261-3.

Wyllie DH, Crook DW, Peto TE. (2006). Mortality after Staphylococcus aureus bacteremia in two hospitals in Oxfordshire, 1997-2003: cohort study. BMJ. 333(7562):281.